Analysis of Linear Features Mapped in Landsat Thematic Mapper and Side-Looking Airborne Radar Images of the Reno 1° by 2° Quadrangle, Nevada and California: Implications for Mineral Resource Studies

Lawrence C. Rowan and Timothy L. Bowers

Abstract

Linear tonal features, which reflect topographic and lithologic differences, were mapped in Landsat Thematic Mapper (TM) and side-looking airborne radar (SLAR) images of the Reno 1° by 2° quadrangle, Nevada and California; combined into a single data set; and compared to the distribution of known Tertiary Au-Ag vein mineralization. The results of analyses of orientation and areal density show that in most areas the linear features are expressions of geologic structures that controlled the mineralization. However, the variability of the spatial correspondence of the two linear features attributes with mines necessitated ranking orientation and areal density values for incorporation into a numerical mineral assessment model.

The results show that the combined spatial resolution of the TM and SLAR images permits delineation of structures that controlled Tertiary precious-metal mineralization in this area. However, the tonal expression of some important structures may be below the resolution limit. Other factors that contribute to the variability of the results are the unknown age of linear features, illumination-induced biases, and shadowing in high-relief terrain.

Introduction

The main objective of most mineral resource studies is to delineate areas according to their potential for specific mineral-deposit types. In the U.S. Geological Survey's (USGS) National Mineral-Resource Assessment Program (NAMRAP), analysis of remotely sensed data has been used extensively to augment conventional geologic, geophysical, and geochemical methods. Maps showing the distribution of hydrothermally altered rocks as interpreted from laboratory and field analyses of Landsat images (e.g., Rowan and Purdy, 1984; Rowan and Segal, 1989; Segal and Rowan, 1989; Rowan *et al.*, in press) are especially useful because the presence of these rocks is clearly indicative of hydrothermal activity, which may result in economic mineralization.

Analysis of linear features mapped in Landsat images has also been used widely in mineral resource studies (Rowan and Purdy, 1985; Purdy and Rowan, 1990; Rowan *et al.*, 1991), but the results typically are difficult to integrate into mineral assessment models (Cox and Singer, 1986). Numerous factors contribute to the complexity of this problem. First, linear features are assumed to be topographic and tonal manifestations of structural features or structurally controlled features, such as dikes, but some may reflect a more general structural fabric, such as joints and foliation. Second, the spatial resolution of satellite images, particularly the Landsat Multispectral Scanner images (79 m), may be inadequate to consistently detect the surface manifestations of structural features that controlled certain deposits, such as epithermal veins. Although these images are useful for delineating regional structural zones that may have influenced formation of metal deposits (Lathram and Raynolds, 1977; Raines, 1978; Warner, 1978; Rowan and Wetlaufer, 1981), delineation of specific potentially mineralized areas is limited by the large dimensions of these inferred structural zones relative to the typical size of most mineral deposits (Gilluly, 1976). Finally, many analyses of linear features are conducted without consideration of the type or the ages of the mineralization or the linear features. The combination of these factors results in highly variable spatial correspondence between linear features and known mineralization within most areas (Rowan and Purdy, 1984; Rowan and Purdy, 1985; Purdy and Rowan, 1990; Rowan *et al.*, 1991), which limits the value of linear-feature analysis to mineral assessment.

During the 1980s, the spatial resolution of satellite images improved to 30 m for Landsat Thematic Mapper (TM) images, 10 and 20 m for SPOT (Satellite Pour l'observation de la Terre) images, and 5 m for Russian nondigital (photographic) images. In addition, the U.S. Geological Survey has acquired side-looking airborne radar (SLAR) images with approximately 12-m resolution for approximately 40 percent of the United States. Detection of linear features that are directly related to fractures, dikes, and hydrothermally altered rocks may be possible using the higher resolution TM and

U.S. Geological Survey, MS 927, National Center, Reston, VA 22092.

Photogrammetric Engineering & Remote Sensing,
Vol. 61, No. 6, June 1995, pp. 749–759.

0099-1112/95/6106-749$3.00/0

SLAR images, but this type of evaluation has not been conducted previously for a large, highly mineralized area where the orientations of structurally controlled deposits have been well documented.

Objectives

An opportunity to conduct an evaluation of TM- and SLAR-derived linear features occurred when John *et al.* (1993) completed the mineral-resource assessment of the Reno 1° by 2° quadrangle, Nevada and California. The main objective of our study was to evaluate the spatial correspondence between linear features derived from Landsat TM and SLAR images and known metallic epithermal-vein deposits. The adequacy of the spatial resolution of these images for detecting structural features that controlled mineralization was of particular interest. A secondary objective was determination of the geologic and image characteristics that cause variability in the spatial correspondence of linear features and mines and prospects within the study area.

Analysis of Linear Features

Procedures

Tonal linear features mapped in the TM and SLAR images are mainly straight to slightly curvilinear topographic features, such as segments of drainages, ridges, and escarpments, but in a few areas they reflect lithologic contrast (O'Leary *et al.*, 1976). Two attributes of linear features were considered: (1) orientation with respect to the trend of structural features known to control the formation of the precious-metal vein deposits (control orientation) and (2) areal density. Three databases were used in the analysis: (1) mapped linear features (Plate 1a), (2) locations of mines and prospects (Plate 1b), and (3) areas mapped by John *et al.* (1993) as favorable for epithermal gold-silver deposits (Plates 1a and 1b). The linear features were mapped visually in 1:250,000-scale TM band 3 and band 4 images and a SLAR image mosaic. The TM and SLAR linear features were digitized as individual maps and subsequently combined to avoid digitization of the same feature twice.

The locations of mines and prospects in the Reno quadrangle were extracted from the USGS Mineral-Resource Data System (MRDS) and updated on the basis of a list provided by John and Sherlock (1991). The sources for this updated list were MRDS, county reports, and field investigations. The final list contains 380 locations and served as our master database of mines and prospects.

The mineral assessment of the Reno quadrangle by John *et al.* (1993) delineated 21 tracts judged favorable for the occurrence of undiscovered Tertiary precious-metal epithermal vein deposits. Selection of these tracts (Plates 1a and 1b) involved an integrated analysis of several factors, including locations of mines and prospects, igneous centers and (or) intrusions, hydrothermally altered rocks, and geochemical anomalies, as well as published descriptions (John *et al.*, 1993). The linear features were mapped prior to the mineral assessment of the quadrangle but were not analyzed until the assessment was completed.

Digital spatial analysis of the linear features was performed using the Geographic Resource Analysis Support System (GRASS) (Anonymous, 1988) geographic information system (GIS) software. The linear features, mines and prospects, and favorable tract data sets were projected into the Universal Transverse Mercator (UTM) coordinate system. The projected data were then converted to a raster, or grid, format with each cell having a ground resolution of 100 m.

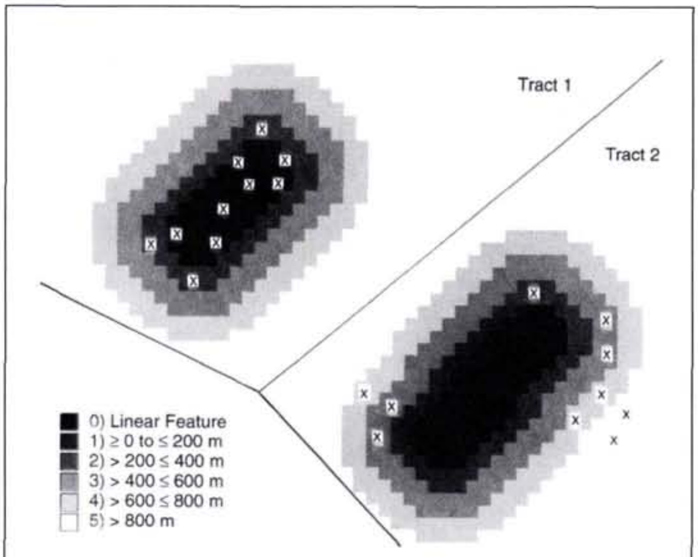

Figure 1. Hypothetical example of two tracts with northeast-trending linear features surrounded by increasingly larger buffer zones: 0 (coincident), >0 to ≤200 m, >200 to ≤400 m, >400 to ≤600 m, and >600 to ≤800m. X indicates locations of mines.

Four pre-analysis processing steps produced the intermediate data sets needed for the quantitative spatial analysis. First, the 180° azimuthal range was divided into twelve 15° sectors. Each linear feature was assigned to one of these twelve subsets. Linear feature directions were determined using the UTM coordinate system.

Next, linear feature proximity maps were produced for each of the 12 subsets. A proximity map was constructed by building a concentric set of four, 200-m-wide buffer zones around each linear feature (Figure 1).

Certain deposit types (e.g., Comstock epithermal vein, polymetallic vein, and hot-spring Au-Ag) are commonly associated with vein or fracture systems (Cox and Singer, 1986). Assuming that linear features are surface expressions of vertically extensive vein, fracture, or fault systems, we were interested only in those mines and prospects whose mineralization was vein controlled. The third pre-analysis step produced a subset of 286 vein-controlled master mines and prospects from the master data base (Plate 1b).

The final step was to prepare a map of linear feature density by counting the number of linear features within a 27 by 27 neighborhood (2.7 by 2.7 km) of each grid cell. A 7 by 7 averaging filter was used to smooth the data and produce a "contoured" surface.

Orientation

The terms defined below are used frequently in our discussion of the orientation analysis:

- *control features* – linear features whose oriention corresponds to the trend of structural features that controlled emplacement of epithermal vein deposits (John *et al.*, 1993);
- *noncontrol features* – linear features whose orientation does

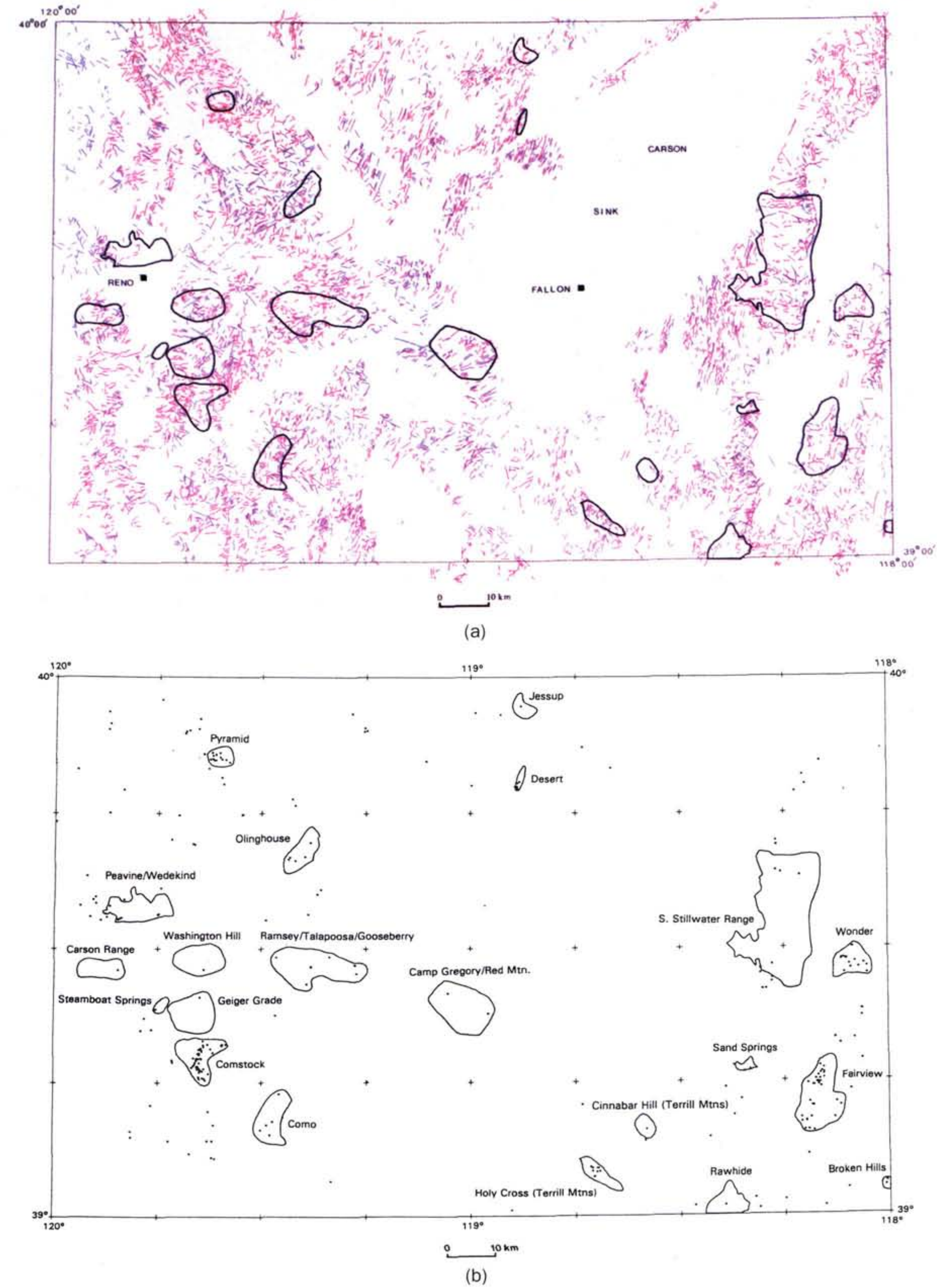

Plate 1. Maps of the Reno 1° by 2° quadrangle, Nevada and California, showing the favorable tracts (closure areas) for undiscovered precious-metal epithermal vein deposits (John *et al.*, 1993). (a) Linear features mapped in Landsat Thematic Mapper (TM) (red) and side-looking airborne radar (SLAR) (blue) images. (b) Location of mines and prospects that exploited vein deposits. Names of tracts are referred to in the text.

TABLE 1. NUMBER OF MINES AND CORRESPONDING PERCENTAGE OF MINES ENCOMPASSED BY BUFFER ZONES IN TRACTS 1 AND 2 SHOWN IN FIGURE 2 AND THE MAXIMUM BUFFER. THE MAXIMUM BUFFER HAS THE HIGHEST PERCENTAGE OF ENCOMPASSED MINES.

Tract number	Buffer dimension, in metres	Number of mines encompassed	Percent of mines encompassed	Maximum buffer
1	0 (coincident)	2	20	
	>0 to ≤200	5	50	X
	>200 to ≤400	3	30	
	>400 to ≤600	0	0	
	>600 to ≤800	0	0	
	>800	0	0	
		Total 10	Total 100	
2	0 (coincident)	0	0	
	>0 to ≤200	0	0	
	>200 to ≤400	1	10	
	>400 to ≤600	4	40	X
	>600 to ≤800	3	30	
	>800	2	20	
		Total 10	Total 100	

not correspond to that of structures that controlled vein mineralization;
- *azimuthal sector* – a single 15° range; and
- *azimuthal range* – a collection of azimuthal sectors, such as N0°-45°E

The association of epithermal vein deposits with fractures and fracture-controlled intrusive bodies is widely recognized, but documentation of the orientation of these control structures for a large mineralized region, such as the Reno quadrangle, commonly is lacking. John *et al.* (1993) documented the orientation of structures that controlled deposition of the precious-metal deposits in 19 of the 21 tracts.

In most tracts, the orientation of controlling structural features is stated in general terms, such as "northeast-trending faults," "north-northeast shear zone," "west-northwest veins," etc. (John *et al.*, 1993). We expanded the control azimuthal range by ±15° about the stated orientation to ensure that linear features possibly reflecting structural control were included in the orientation analysis. For example, we analyzed N0°-30°E for north-northeast-oriented control structures; N30°-60°E for northeast-trending structures; and N75°-90°E and N75°-90°W for west-trending structures. Specific orientations are given for the Camp Gregory/Red Mountain (N60°E), Wonder (N25°W), and Broken Hills (N30°W) tracts. Control structures were not documented for the Jessup and Desert tracts; therefore, these tracts are not included in this analysis. In the Camp Gregory/Red Mountain tract, N45°-75°E was used to span the N60°E-trending faults and hydrothermal breccia zones (John *et al.*, 1993). John *et al.* (1993) also noted the presence of northeast- and north-northwest-trending faults in the Camp Gregory/Red Mountain tract, and so the control-azimuthal ranges analyzed were N30°-75°E and N0°-30°W. In the Wonder tract, we analyzed the N15°-90°W range to encompass the N25°W-trending fault noted by John *et al.* (1993) and the N45°-90°W-oriented veins mapped by Willden and Speed (1974).

We realize that, in a study such as this, imprecisions may be introduced into the data collection and analysis. Three sources of imprecision are recognized: (1) the linear features were digitized manually at 1:250,000 scale, which may have been too coarse for small orientation variations; (2) as a result of using broad azimuthal ranges to represent controlling structure, more linear features may be included in control orientations than is appropriate; and (3) because of UTM grid convergence within the Reno quadrangle, using UTM coordinates for directional determination introduced an error of between 1° and 2° during the calculation of linear feature orientation.

Proximity Analysis

Proximity is an important factor in the analysis of the spatial association of linear features with known mineralization. Proximity can be evaluated by examining the percentage of mines encompassed by each 200-m-wide buffer zone for each of the 12 azimuthal sectors. The procedure used in this study to make the basic proximity computations is illustrated by Figure 1. In this hypothetical example, one northeast-trending linear feature and ten mines are present in tracts 1 and 2. The number of mines present in each of the buffer zones and the corresponding percentage of encompassed mines are compared for these tracts in Table 1. In tract 1, all the mines lie within 400 m of the linear feature; in contrast, in tract 2, only 10 percent of the mines are encompassed by buffers between 0 and 400 m, whereas 20 percent lie outside of the four buffers. Thus, the mines are closer to the linear features in tract 1 than in tract 2. The buffer dimensions that encompass the maximum percentage of mines are 0 to 200 m in tract 1 and 400 to 600 m in tract 2.

For each of the 19 favorable tracts, we calculated the percentage of mines encompassed by each buffer zone surrounding the control features. The resulting values were examined to identify the buffer encompassing the largest percentage of mines, referred to as the *maximum buffer* (Table 2a). As a control on our study, we also calculated the percentage of mines within the buffers surrounding noncontrol features (Table 2b). Where two buffer sizes yielded the maximum values, the largest buffer was used in the calculations. Note that the >800 m buffer was not included as one of the maximum buffer dimensions, because this includes the remainder of the map area.

The difference between the percentage of mines encompassed by the maximum buffers surrounding control and noncontrol linear features is referred to as the **normalized orientation index** (NOI). NOI is computed as follows:

$$\mathrm{NOI} = \frac{1}{N_c}\sum_{i=1}^{\max} x_i - \frac{1}{N_n}\sum_{i=1}^{\max} x_i$$

where x is the percentage of mines within a specified buffer zone; i is the buffer number (1 indicates coincidence with

TABLE 2a. PERCENTAGE OF MINES ENCOMPASSED BY EACH BUFFER FOR ALL CONTROL-AZIMUTHAL RANGES. MAXIMUM PERCENTAGE OF MINES INDICATED BY BOLD AND UNDERLINED TYPE. NUMBER OF AZIMUTHAL SECTORS FOR CONTROL ORIENTATIONS SHOWN IN THIRD COLUMN.

Tract Name	No. of mines within tract	No. of azimuthal sectors	Buffer Dimensions, in Metres: 0	> 0 to ≤ 200	200 to ≤ 400	400 to ≤ 600	600 to ≤ 800	> 800
Broken Hills	2	2	0	0	0	0	0	100
Camp Gregory/Red Mountain	2	5	50	0	**50**	0	0	0
Carson Range	1	5	0	0	**100**	0	0	0
Cinnabar Hill/Terrill Mts.	1	2	0	0	0	0	100	0
Como	5	7	0	20	20	**40**	0	20
Comstock	52	3	6	21	**21**	19	2	31
Fairview	33	5	6	9	**19**	15	12	39
Geiger Grade	1	2	0	0	0	0	0	100
Holy Cross/Terrill Mountains	9	2	0	11	**33**	22	11	23
Olinghouse	5	2	20	**40**	0	20	0	20
Peavine/Wedekind	8	4	13	0	**37**	13	0	37
Pyramid	12	5	0	25	17	17	**32**	9
Ramsey/Talapoosa/Gooseberry	8	6	0	12	12	**63**	0	13
Rawhide	1	6	0	0	0	0	**100**	0
Sand Springs	2	2	**100**	0	0	0	0	0
Southern Stillwater Range	4	2	0	25	**50**	25	0	0
Steamboat Springs	2	2	0	0	0	0	0	100
Washington Hill	1	2	0	0	0	0	0	100
Wonder	17	5	0	**35**	18	6	12	29

linear feature); maxbuf is the number of the buffer that contains the maximum percentage of mines; N_c is the number of 15° sectors that contain the directions of the control linear features; and N_n is the number of 15° sectors that contain the noncontrol linear features.

Table 3 lists NOI values for each of the 15 favorable tracts for which the maximum buffer could be determined. All the NOI values are positive, except for the Como tract. Positive values show that control-oriented linear features better correspond to known mineralization than do noncontrol features. The maximum buffer dimension could not be determined in four tracts because of the lack of correspondence of linear features with mines, which are sparse in these tracts.

The results of the orientation analysis indicate that the spatial resolutions of the Landsat TM and SLAR images are adequate to detect topographic and tonal expressions of

TABLE 2b. PERCENTAGE OF MINES ENCOMPASSED BY EACH BUFFER FOR ALL NONCONTROL-AZIMUTHAL RANGES. MAXIMUM PERCENTAGE OF MINES FOR CONTROL-ORIENTED FEATURES INDICATED BY BOLD TYPE AND UNDERLINE (TABLE 2A). COLUMN THREE SHOWS THE NUMBER OF NONCONTROL AZIMUTHAL SECTORS IN EACH TRACT.

Tract Name	No. of mines within tract	No. of azimuthal sectors	Buffer Dimensions, in Metres: 0	> 0 to ≤ 200	200 to ≤ 400	400 to ≤ 600	600 to ≤ 800	> 800
Broken Hills	2	10	0	0	50	0	50	0
Camp Gregory/Red Mountain	2	7	50	0	**0**	0	0	50
Carson Range	1	7	100	0	**0**	0	0	0
Cinnabar Hill/Terrill Mts.	1	10	0	0	0	0	100	0
Como	5	5	0	60	0	**0**	0	40
Comstock	52	9	2	21	**25**	29	13	10
Fairview	33	7	3	27	**15**	12	15	27
Geiger Grade	1	10	0	0	100	0	0	0
Holy Cross/Terrill Mountains	9	10	11	78	**11**	0	0	0
Olinghouse	5	10	0	**0**	40	40	20	0
Peavine/Wedekind	8	8	0	37	**25**	0	0	38
Pyramid	12	7	17	41	17	17	**8**	0
Ramsey/Talapoosa/Gooseberry	8	6	0	37	38	**12**	13	0
Rawhide	1	6	0	0	0	0	**0**	100
Sand Springs	2	10	**0**	50	0	50	0	0
Southern Stillwater Range	4	10	25	0	**25**	25	25	0
Steamboat Springs	2	10	0	50	50	0	0	0
Washington Hill	1	10	0	100	0	0	0	0
Wonder	17	7	0	**18**	18	35	6	23

TABLE 3. NORMALIZED ORIENTATION INDEX (NOI), IN PERCENT, MAXIMUM BUFFER DIMENSION (TABLE 2), NUMBER OF MINES WITHIN EACH FAVORABLE TRACT. POSITIVE NOI VALUES INDICATE THAT CONTROL FEATURES CORRESPOND TO KNOWN MINERALIZATION BETTER THAN NONCONTROL FEATURES. NOI WAS NOT DETERMINED FOR TRACTS THAT LACK A MAXIMUM BUFFER.

Tract name	NOI, Percent	Maximum buffer dimension, in metres	Number of mines within tract
Broken Hills	—	none	2
Camp Gregory/Red Mountain	+13	> 200 to ≤ 400	2
Carson Range	+6	> 200 to ≤ 400	1
Cinnabar Hill/Terrill Mountains	+40	> 600 to ≤ 800	1
Como	−1	> 400 to ≤ 600	5
Comstock	+11	> 200 to ≤ 400	52
Fairview	+0.4	> 200 to ≤ 400	33
Geiger Grade	—	none	1
Holy Cross/Terrill Mountains	+12	> 200 to ≤ 400	9
Olinghouse	+30	> 0 to ≤ 200	5
Peavine/Wedekind	+6	> 200 to ≤ 400	8
Pyramid	+4	> 600 to ≤ 800	12
Ramsey/Talapoosa/Gooseberry	+2	> 400 to ≤ 600	8
Rawhide	+17	> 600 to ≤ 800	1
Sand Springs	+50	0 (coincident)	2
Southern Stillwater Range	+33	> 200 to ≤ 400	4
Steamboat Springs	—	none	2
Washington Hill	—	none	1
Wonder	+4	> 0 to ≤ 200	17

many of the structural features that controlled the formation of epithermal vein deposits in the Reno 1° by 2° quadrangle. In addition, the resulting NOI values can be used as a means of expressing the relative importance of the linear features in and adjacent to the favorable tracts. The procedure followed in the analysis could be used in other areas for evaluating linear features derived from images that have similar or higher spatial resolutions, and where the orientation of controlling structures is known or could be determined.

Areal Density

Areal density is a potentially important linear feature attribute, because high density might indicate fractures that might be favorable for vein mineralization (Jerome and Cook, 1967). Some of the favorable tracts clearly display high areal density levels, especially the Como, Olinghouse, Holy Cross/Terrill Mountains, and Pyramid tracts (Plate 1b). In contrast, the Wonder, Fairview, Rawhide, and Cinnabar Hill/Terrill Mountains tracts exhibit low to moderate linear feature density. Thus, the spatial correspondence between linear feature density and the tracts is highly variable. A systematic analysis was conducted to determine the spatial relationship between density and known mineralization within the tracts.

The areal density of linear features was analyzed by first identifying a range of areal density that corresponds to a high percentage of all mines shown in Plate 1b and, then, evaluating the percentage of mines encompassed by this range within each tract. Because the association of known mineralization with small concentrations of linear features is of particular interest, we examined the percentage of encompassed mines as a function of the percentage of area covered by linear features over the entire range of areal density. The encompassed mines/encompassed area ratio, which is referred to as the *normalized density* (Rowan *et al.*, 1991), is high in the areal density range from 22 to 29 and moderately high in the range from 16 to 21 (Figure 2). The ≥16 areal density range was selected for analysis because the normalized density over this range is substantially higher than that of the <16 areal density range.

Plate 2 shows the spatial relationships between the ≥16 to 36 areal density range, mines, and tracts. The Sand Springs, Washington Hill, Camp Gregory/Red Mountain, Holy Cross/Terrill Mountains, Como, Olinghouse, and Desert tracts have a large percentage of mines encompassed by the areas of high linear feature density. This spatial relationship

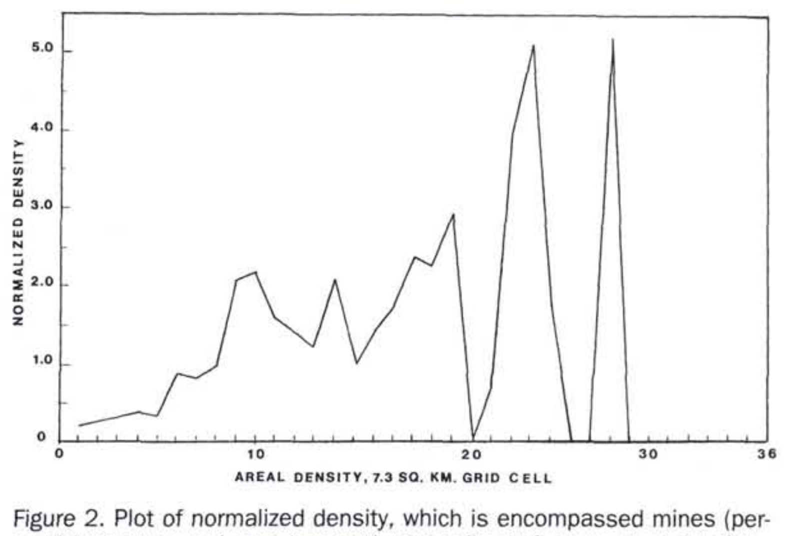

Figure 2. Plot of normalized density, which is encompassed mines (percent)/encompassed area (percent) versus linear feature areal density. The grid cell dimension was 2.7 by 2.7 km.

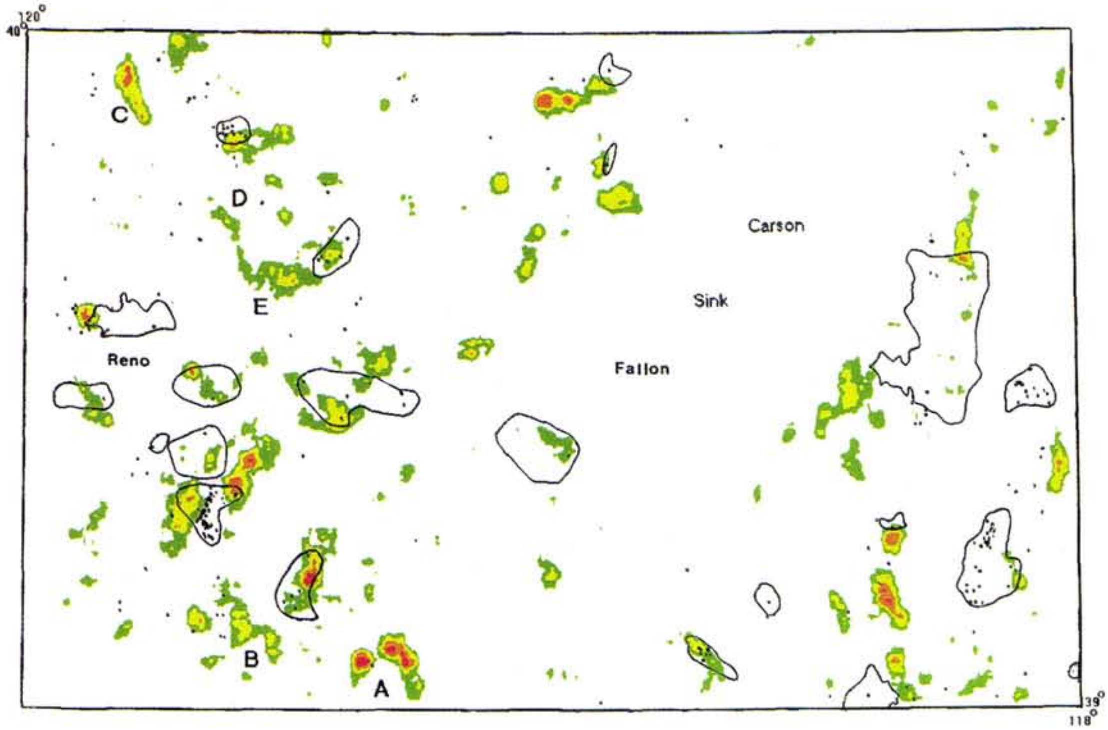

Plate 2. Map of the Reno 1° by 2° quadrangle, Nevada and California, showing the favorable tracts for undiscovered precious-metal epithermal vein deposits (John *et al.*, 1993) and the 16 to 36 range of areal density of linear features. Squares indicate mines and prospects that exploited precious-metal vein deposits. Areas A to E are discussed in the text. Density ranges are green — 16 to 20; yellow — 21 to 25; pink — 26 to 30; and red — 31 to 36.

suggests that mineralization may be associated with numerous fractures within these tracts. In contrast, the percentage of encompassed mines is relatively low in the Comstock and Fairview tracts and is zero in several tracts (Figure 3).

Some of the high-density areas correspond to tracts that were delineated for other deposit types, which are not considered in this study. For example, areas A and B in the southwestern part of the Reno quadrangle (Plate 2) correspond to large parts of the Singatse/Bucksin and Northern Pine Nut porphyry areas, respectively (John *et al.*, 1993). Other areas of high density correspond to major fault zones. In the northwestern corner of the quadrangle, the northwest-trending high density areas (C and D, Plate 2) are related to numerous faults within the northwest-trending Walker Lane fault zone (Albers, 1967; Rowan and Wetlaufer, 1981). The roughly 90° bend in the concentration pattern south of area D (E, Plate 2) marks the intersection of the Walker Lane faults and the northeast-trending faults in the Pah Rah Range (Bonham, 1969).

Application to Mineral Resource Studies

Linear feature orientation and areal density data can be used in both the initial and final stages of mineral resource studies. In the initial stage, when favorable ground has been tentatively delineated mainly through evaluation of the areal distributions of mines, information on the areal density of linear features is useful for defining and modifying the initial boundaries and, perhaps, selecting additional potential sites. If the orientation of controlling structural features is known, the tracts can be refined further.

As analysis and synthesis of field and laboratory data allow refinement of the favorable tract locations and boundaries, linear feature orientation and areal density data should be ranked for incorporation into numerical assessment models. In most site assessment models, each element (host rock, hydrothermally altered rocks, faults, etc.) is assigned a value, and the proportion of the value applied to a site is determined by the strength with which the element is expressed. For some factors, such as hydrothermally altered rocks, the expression is typically binary (present or absent). Other elements have more variable strength of expression and are weighted accordingly.

In the Reno quadrangle, if linear features were assigned a deposit model value of 6 in a hypothetical epithermal vein deposit model, we would divide this value equally between the NOI and linear feature areal density. Then, the NOI and areal density would be ranked for each tract such that high = 3, moderate = 2, low = 1, and unranked = 0. The resulting scores would be summed to determine the deposit model values. The results of this procedure are shown in Table 4. The NOI is ranked highest for the Sand Springs, Cinnabar Hill/Terrill Mountains, Southern Stillwater Range, and Olinghouse tracts. The medium ranked tracts are the Comstock, Rawhide, Camp Gregory/Red Mountain, and Holy Cross/Ter-

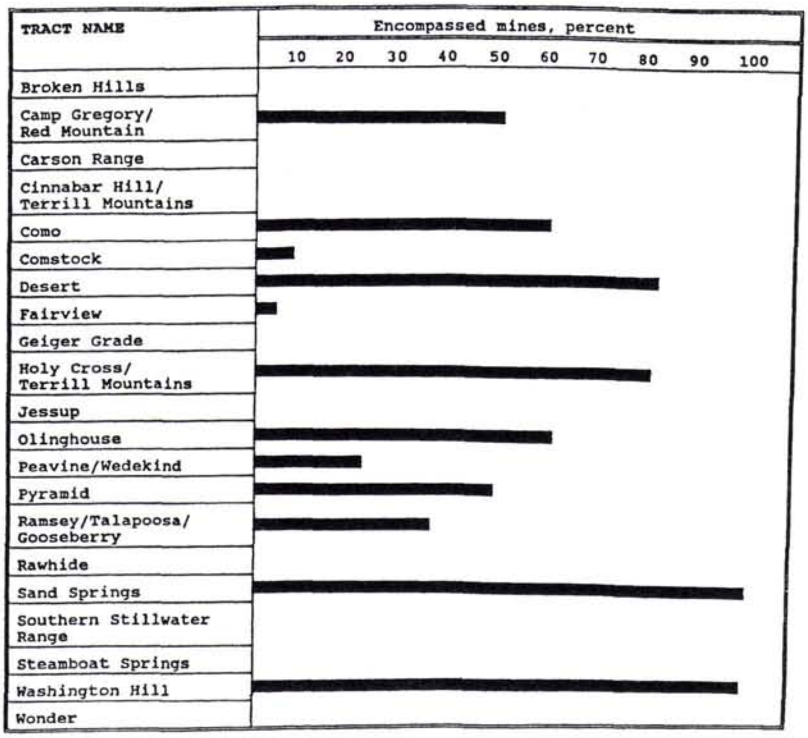

Figure 3. Percentage of mines encompassed within tracts by high-density area shown in Plate 2. Absence of line indicates that no mines were encompassed.

rill Mountains tracts. The Pyramid, Ramsey/Talapoosa/Gooseberry, Wonder, Peavine/Wedekind, and Carson Range tracts are ranked low, and the other tracts are very low.

Ranking the areal density results would be based on the percentage of mines encompassed within the tract (Figure 3; Table 4). In Table 4, the tracts have been placed into the following levels according to the percentage of mines encompassed by the high areal density range: (1) high - Washington Hill, Como, Olinghouse, Desert, Holy Cross/Terrill Mountains, and Sand Springs; (2) medium - Pyramid, Peavine/Wedekind, Ramsey/Talapoosa/Gooseberry and Camp Gregory/Red Mountain; (3) low - Comstock and Fairview; and (4) unranked - the Carson Range, Steamboat Springs, Geiger Grade, Jessup, Wonder, Cinnabar Hill/Terrill Mountains, Southern Stillwater Range, Rawhide, and Broken Hills tracts.

The deposit model values are highest (6 to 4) for the Sand Springs, Olinghouse, Holy Cross/Terrill Mountains, and Camp Gregory/Red Mountain tracts; and the deposit model value is 3 for the Pyramid, Peavine/Wedekind, Washington Hill, Comstock, Como, Desert, Ramsey/Talapoosa/Gooseberry, Cinnabar Hill/Terrill Mountain, and Southern Stillwater Range tracts (Table 4). These values could be used directly in an assessment model for this deposit type. However, care must be exercised in evaluating the areal density data, because a high percentage of mines may be encompassed by linear features that are not related to the mineralization.

This approach is useful for aiding initial delineation of tracts, subsequent refinement of boundaries, and identification of promising areas within and near tracts, but identification of potential sites outside of the tracts requires a different strategy. One such strategy is to use a GIS to evaluate the orientation and density data concurrently.

The areas between the Comstock and Como tracts and near the Geiger Grade and Washington Hill tracts are described by John *et al.* (1993) as having conditions that are permissive for the occurrence of undiscovered precious-metal vein deposits of Tertiary age. Linear features trending N0°-45°E were selected for evaluating the permissive area because they correspond to mines in all four tracts (Plate 1). In Plate 3, the densities of these linear features are contoured, and the areas of high density of all linear features (Plate 2) are outlined in red. In general, the high-density areas coincide with concentrations of features trending N0°-45°E. A notable exception is along the western margin of the Comstock tract, where high areal density only partially corresponds to a small area of moderately dense linear features trending N0°-45°E. This area is dominated by northwest- to west-northwest-trending faults that did not control the mineralization (Vikre, 1989).

The largest area within the permissive region where both linear feature attributes are concentrated extends north-northeastward from the northeastern corner of the Comstock tract (Plate 3). The N0°-45°E-trending linear features reflect a prominent topographic grain that is evident in this area. Few faults are mapped in this area (Thompson, 1956), hydrothermally

TABLE 4. RELATIVE RANK OF TRACTS BASED ON NORMALIZED ORIENTATION INDEX (NOI) AND AREAL DENSITY OF LINEAR FEATURES (TABLE 3, FIGURE 5). VALUES IN PARENTHESIS FOR ORIENTATION AND AREAL DENSITY RANKS ARE HIGH (H) = 3, MEDIUM (M) = 2, LOW (L) = 1, AND VERY LOW (VL) = 0. THE DEPOSIT MODEL VALUE IS THE SUM OF THE ORIENTATION AND AREAL DENSITY VALUES. NA, *NOT* APPLICABLE AS CONTROL STRUCTURES WERE NOT DOCUMENTED FOR THE DESERT AND JESSUP TRACTS.

	Orientation		Areal density		
Tract name	NOI (percent)	Rank	Percent of mines	Rank	Deposit model value
Broken Hills	—	VL-(0)	0	VL (0)	0
Camp Gregory/Red Mountain	13	M (2)	50	M (2)	4
Carson Range	6	L (1)	0	VL (0)	1
Cinnabar Hill/Terrill Mountains	40	H (3)	0	VL (0)	3
Como	−1	VL-(0)	60	H (3)	3
Comstock	11	M (2)	10	L (1)	3
Desert	NA	—	80	H (3)	3
Fairview	0.4	VL (0)	3	L (1)	1
Geiger Grade	—	VL-(0)	0	VL (0)	0
Holy Cross/Terrill Mountains	12	M (2)	78	H (3)	5
Jessup	NA	—	0	VL (0)	0
Olinghouse	30	H (3)	60	H (3)	6
Peavine/Wedekind	6	L (1)	25	M (2)	3
Pyramid	4	L (1)	50	M (2)	3
Ramsey/Talapoosa/Gooseberry	2	L (1)	38	M (2)	3
Rawhide	17	M (2)	0	VL (0)	2
Sand Springs	50	H (3)	100	H (3)	6
Southern Stillwater Range	33	H (3)	0	VL (0)	3
Steamboat Springs	—	VL-(0)	0	VL (0)	0
Washington Hill	—	VL-(0)	100	H (3)	3
Wonder	4	L (1)	0	VL (0)	1

altered rocks are limited to the southern part of this zone (Rowan *et al.*, in press), and no mines are documented by John and Sherlock (1991).

The area north of the Como tract is also characterized by coincidence of these two linear feature attributes (Plate 3), but mines (John and Sherlock, 1991) and hydrothermally altered rocks (Rowan *et al.*, in press) have not been reported in this area. The area about 10 km west of the Como tract might also be of interest.

Sources of Spatial Correspondence Variation

Several sources may contribute to the variations observed in the spatial correspondence of linear feature areal density to favorable tracts and control orientation to known mineralized sites within the tracts. The following sources appear to be most important: (1) linear features may post-date mineralization, (2) structural-control data are of variable quality, (3) image spatial resolution may be too low, (4) illumination conditions cause some features to be obscured, and (5) cultural features may obscure linear features. Careful field studies are required to date linear features and mineralization and to identify structural controls. The other factors are related to image quality and are discussed below. Factors such as electronic noise and cloud and/or snow cover were not problems with the TM and SLAR data used in this study.

Spatial Resolution

The adequacy of spatial resolution of a particular image depends on the expressions of the geologic structures of interest. According to the published descriptions, nearly all the veins within the favorable tracts are smaller than the spatial resolutions of the SLAR and TM images. However, many fault escarpments with which the veins are associated have sufficient topographic relief to be detected in these images, and some of the zones of hydrothermally altered rocks that border the veins are large enough to be detected with the given sensor resolution. The expressions of at least some of the control structures in 1:24,000-scale topographic maps are evident in the Pyramid, Comstock, Como, Olinghouse, Camp Gregory/Red Mountain, Wonder, Southern Stillwater Range, Holy Cross/Terrill Mountains, Fairview, and Sand Springs tracts. Generally, linear zones of hydrothermally altered rocks correspond to the orientations of the main control structures in the Pyramid, Olinghouse, Camp Gregory/Red Mountain, and Wonder tracts (Rowan *et al.*, in press). Except for the Fairview and Holy Cross/Terrill Mountain Tracts, there is generally a good spatial correspondence between the control-structure azimuthal ranges and mineralized sites. These structures may be detectable in aerial photographs, which have substantially higher spatial resolution than the images used in this study.

Illumination Conditions

The areal density of linear features is substantially higher in the map of TM-derived features than in the SLAR map (Plate 1a). This difference is due mainly to the masking of linear features by much more extensive shadows in the SLAR image mosaic than in the TM images. Because of the low-angle westward illumination (average depression angle = 16°) of the SLAR image mosaic, extensive shadows mask areas on west-facing slopes in high-relief areas. Shadows also occur on the northwest-facing slopes in the TM images, but they obscure fewer linear features than in SLAR images. The Fairview tract exemplifies the importance of illumination ge-

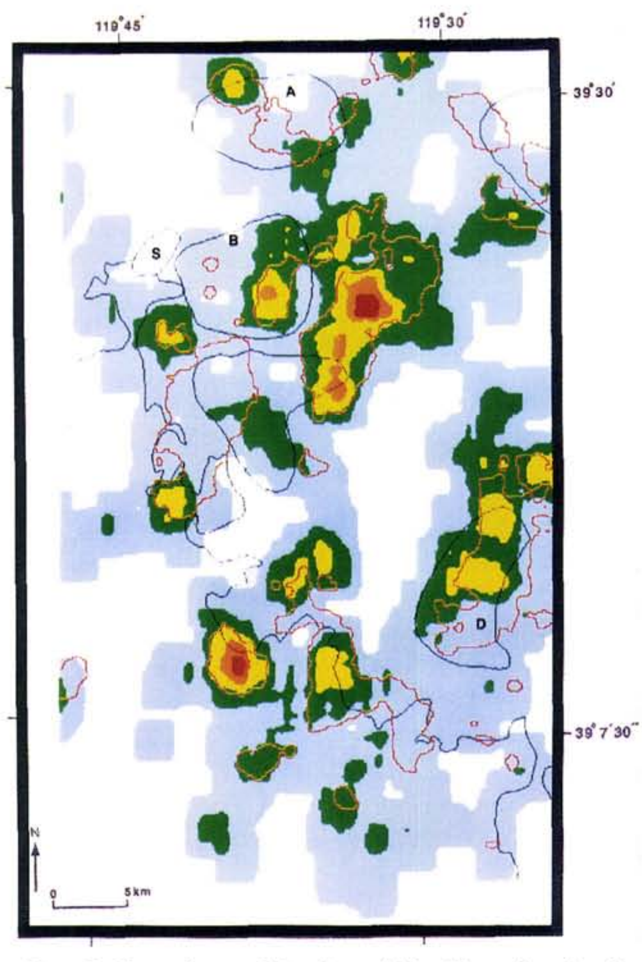

Plate 3. Map of part of the Reno 1° by 2° quadrangle, Nevada and California, showing part of the area considered permissive for precious-metal vein deposits (John *et al.*, 1993). Color contours (contour interval = 4) indicate density of features trending N0°-45°E. Red lines enclose areas where areal density of all linear features is high (Plate 2). Light-black lines enclose favorable tracts (Plate 1): A, Washington Hill; B, Geiger Grade; C, Comstock; D, Como; and S, Steamboat Springs. Heavy black line locates southwestern boundary of the permissive area (John *et al.*, 1993).

ometry and topographic configuration. The mountain range trends generally north-northeast, and maximum topographic relief on the west side is about 1,000 m. Most of the precious-metal vein deposits are situated on the western slope (Willden and Speed, 1974), where extensive shadows obscure linear features, especially in the SLAR mosaic.

Strike-frequency plots of the TM and SLAR linear features are strongly influenced by the illumination directions that prevailed during acquisition of the images. In the TM plot, the strike-frequency minimum at N45°-60°W includes the solar illumination azimuths of the images (Figure 4). The frequencies of linear features that generally parallel the solar illumination direction are depressed because of the lack of topographic shadowing. The SLAR strike-frequency plot displays a minimum in the N75°W to N75°E range (Figure 4), which includes the illumination direction (west). Similar relations have been observed in other studies of linear features mapped on these types of images (Purdy and Rowan, 1990; Rowan *et al.*, 1991). Combining the TM and SLAR data sets partially compensates for these illumination biases.

Comparison of the percentage of mines encompassed by the TM- and SLAR-derived linear features further illustrates the importance of illumination direction and the complementary nature of these two data sets. In the 14 tracts where some spatial correspondence is displayed (NOI is positive, Table 4), analysis of TM images provided all or nearly all the control linear features in seven of them. The SLAR mosaic was not the dominant linear feature source in any tract, but numerous features were mapped within the N45°-60°W range in ten tracts, which encompasses the solar illumination azimuth of the TM images. Therefore, the SLAR mosaic provided linear feature information for an azimuthal range that was degraded in the TM images due to the solar azimuth. On the other hand, few linear features were mapped within the N75°-90°E range, which contains the west orientation of the SLAR illumination.

Conclusions

The results of the orientation analysis of linear features show that the spatial resolutions of the TM and SLAR images permit delineation of the topographic and tonal expressions of structural features that influenced the formation of Tertiary precious-metal deposits in the Reno quadrangle. Where the orientation of structures that controlled the mineralization is known, the spatial correspondence of the linear features can be ranked by the difference between the percentage of mines encompassed by the control and noncontrol features. Evaluation of variable buffer dimensions permits refinement of the proximity analysis. Areal density analysis, which does not depend on orientation information, is useful for delineating areas that may be favorable for precious-metal veins. These results can be ranked by comparison of selected density lev-

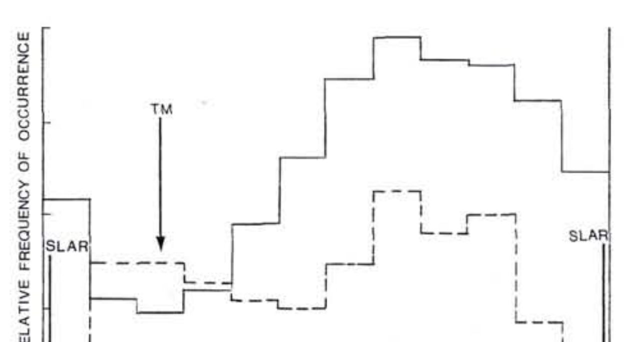

Figure 4. Strike-frequency diagrams of the linear features mapped in Landsat Thematic Mapper (TM) (solid line) and side-looking airborne radar (SLAR) images (broken line) (Plate 1a). Arrows indicate TM and SLAR illumination directions, which were 115° to 123° and 90°, respectively.

els to the distribution of mines or favorable areas that were determined by other methods. Detailed analysis of these linear feature attributes, which is facilitated by using a geographic information system, allows delineation of promising areas within selected tracts, modification of tract boundaries, and perhaps identification of other favorable areas.

The variability of the spatial association of linear features with known precious-metal vein mineralization in the study area is due to spatial resolution limitation, and illumination conditions. Masking of linear features by shadows in SLAR images could be minimized by acquiring data with at least two illumination directions.

Acknowledgments
We thank Melvin Podwysocki and Daniel Knepper for their suggestions for improving this manuscript.

References

Anonymous, 1988. *Geographic Resources Analysis Support System (GRASS) 3.0*, Army Corps of Engineers Construction Engineering Research Laboratory, Champaign, Illinois, 19 p.

Albers, J.P., 1967. Belt of sigmoidal bending and right-lateral faulting in the western Great Basin, *Geol. Soc. America Bull.*, 78:143-156.

Bonham, H.F., Jr., 1969. *Geology and Mineral Resources of Washoe and Storey Counties, Nevada*, Nevada Bureau of Mines and Geology, Bull. 70, 140 p.

Cox, D.P., and D.A. Singer (editors), 1986. *Mineral Deposit Models*, U.S. Geological Survey Bull. 1693, 379 p.

Gilluly, J., 1976. Lineaments - ineffective guides to ore deposits, *Econ. Geol.*, 71:1507-1514.

Jerome, S.E., and D.R. Cook, 1967. *Relation of some Metal Mining Districts in the Western United States to Regional Tectonic Environment and Igneous Activity*, Nevada Bureau of Mines and Geology Bull. 69, 35 p.

John, D.A., and M.G. Sherlock, 1991. *Map Showing Mines and Prospects in the Reno 1° by 2° Quadrangle, Nevada and California*, U.S. Geological Survey Miscellaneous Field Studies Map MF-2154-B, scale 1:250,000, 17 p. text.

John, D.A., J.H. Stewart, J.E. Kilburn, N.J. Silberling, and L.C. Rowan, 1993. *Geology and Mineral Resources of the Reno 1° by 2° Quadrangle, Nevada and California*, U.S. Geological Survey Bull. 2019.

Lathram, E.H., and R.G.H. Raynolds, 1977. Tectonic deductions from Alaska Space Imagery, *First Annual William T. Pecora Memorial Symposium*, U.S. Geological Survey Prof. Paper 1015, pp. 179-192.

O'Leary, D.W., J.D. Friedman, and H.A. Pohn, 1976. Lineament, linear, lineation; some proposed new standards for old terms, *Geol. Soc. America Bull.*, 87:1463-1469.

Purdy, T.L., and L.C. Rowan, 1990. *Map Showing Analysis of Linear Features for Mineral Assessment in the Dillon 1° × 2° Quadrangle, Idaho and Montana*, U.S. Geological Survey Miscellaneous Investigations Series Map I-1803-B, scale 1:250,000, 37 p. text.

Raines, G.L., 1978. Porphyry copper exploration model for northern Sonora, Mexico, *U.S. Geological Survey Journal of Research*, 6(1):51-58.

Rowan, L.C., and T.L. Purdy, 1984. *Distribution of Hydrothermally Altered Rocks, Walker Lake Quadrangle, California and Nevada*, U.S. Geological Survey Miscellaneous Field Studies Map MF-1382-Q, scale 1:250,000.

———, 1985. *Map Showing Analysis of Linear Features in the Wallace 1° × 2° Quadrangle, Idaho - Montana*, U.S. Geological Survey Miscellaneous Field Studies Map MF-1354-H, scale 1: 250,000.

Rowan, L.C., and D.B. Segal, 1989. *Map Showing Locations of Exposures of Limonitic Rocks and Hydrothermally Altered Rocks in the Butte 1° × 2° Quadrangle, Montana*, U.S. Geological Survey Miscellaneous Investigations Series Map I-2050-A, scale 1:250,000.

Rowan, L.C., and P.H. Wetlaufer, 1981. Relation between regional lineament systems and structural zones in Nevada, *American Assoc. Petroleum Geologists Bull.*, 65(8):1414-1432.

Rowan, L.C., B.A. Eiswerth, D.B. Smith, W.J. Ehmann, and T.L. Bowers (in press). *Distribution, Mineralogy, and Geochemistry of Hydrothermally Altered Rocks in the Reno 1° by 2° Quadrangle, Nevada*, U.S. Geological Survey Miscellaneous Field Studies Map MF-2154-D, scale 1:250,000.

Rowan, L.C., C.A. Trautwein, and T.L. Purdy, 1991. *Maps Showing Association of Linear Features and Metallic Mines and Prospects in the Butte 1° by 2° Quadrangle, Montana*, U.S. Geological Survey Miscellaneous Investigations Series Map I-2050-B, scale 1: 250,000.

Segal, D.B., and L.C. Rowan, 1989. *Map Showing Exposures of Limonitic Rocks and Hydrothermally Altered Rocks in the Dillon 1° by 2° Quadrangle, Idaho and Montana*, U.S. Geological Survey Miscellaneous Investigations Series Map I-1803-A, scale 1:250,000.

Thompson, G.A., 1956. Geology of the Virginia City quadrangle, Nevada, *U.S. Geological Survey Bull.* 1042-C, pp. 45-77.

Vikre, P.G., 1989. Fluid-mineral relations in the Comstock Lode, *Econ. Geol.*, 84:1574-1613.

Warner, L.A., 1978. The Colorado Lineament: A middle Precambrian wrench fault system, *Geol. Soc. America Bull.*, 89:161-171.

Willden, R., and R.C. Speed, 1974. *Geology and Mineral Deposits of Churchill County, Nevada*, Nevada Bureau of Mines and Geology, Bull. 83, 95 p.

(Received 22 June 1993; revised and accepted 20 October 1993; revised 4 April 1994)

Lawrence C. Rowan

Dr. Rowan received his B.A. and M.Sc. from the University of Virginia and Ph.D. from the University of Cincinnati. Since joining the U.S. Geological Survey in 1964, he has conducted geological remote sensing research with emphasis on the application of remote sensing to geologic problems. He was Principal Investigator of Landsat 1 and Landsat 2 projects and an Airborne Visible/Infrared Imaging Spectrometer (AVIRIS) study, and a coinvestigator of Landsat Thematic Mapper and Shuttle Multispectral Infrared Radiometer experiments. He is a member of the Advanced Spaceborne Thermal Emission and Reflection radiometer Science Team. He was co-recipient of the 1982 Autometric Award and the William T. Pecora Award from NASA and Department of the Interior. In 1984, he received the Department of the Interior Meritorious Service Award. His current research into the spectral and structural characteristics of alkaline igneous rocks and carbonatites utilizes laboratory and field analysis of AVIRIS and TIMS data to identify lithologies and critical structural features.

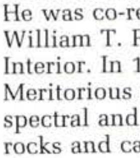

Timothy L. Bowers

Mr. Bowers received both the B.S. degree (1980) and M.S. degree (1987) in geology from Wayne State University, Detroit, Michigan. He is currently with the U.S. Geological Survey, Branch of Geophysics, and is a geology instructor in the Math, Science, and Engineering Division, Northern Virginia Community College. Mr. Bowers is involved in several studies in the application of satellite multispectral and airborne multispectral thermal and hyperspectral visible and near-infrared data for lithologic, mineralogic, and structural mapping. Additional interests include the use of geographic information systems (GIS) technology for the integration and analysis of geologic and remote sensing data.